Available online at www.sciencedirect.com
SCIENCE DIRECT
Geotextiles and Geomembranes 23 (2005) 463–485
Geotextiles and Geomembranes
www.elsevier.com/locate/geotexmem

Analysis of field performance of embankments on soft clay deposit with and without PVD-improvement

Shui-Long Shen[a,*], Jin-Chun Chai[b], Zhen-Shun Hong[c], Feng-Xi Cai[a]

[a]*School of Naval Architecture, Ocean and Civil Engineering, Shanghai Jiao Tong University, 1954 Hua Shan Road, Shanghai 200030, China*
[b]*Institute of Lowland Technology, Saga University, 1 Honjo, Saga 840-8502, Japan*
[c]*Institute of Geotechnical Engineering, Southeast University, Nanjing 210096, China*

Received 19 September 2004; received in revised form 21 May 2005; accepted 31 May 2005

Abstract

This paper presents a case history of the performance of two full-scale test embankments constructed on soft clay deposit in the eastern coastal region of China. One embankment was constructed on natural subsoil and the other was constructed on prefabricated vertical drain (PVD) improved subsoil. The thickness of the soft clay deposit without PVD-improvement was 19 m and with PVD-improved case was 23 m. The PVDs were installed to a depth of 19 m with spacing of 1.5 m in a triangular pattern. Field performance of the two embankments was analyzed using the finite element method. The following influential factors: (i) hydraulic conductivity of subsoil in field and (ii) discharge capacity of PVDs were investigated numerically. The back-analyzed results for the embankment on natural subsoil showed that the hydraulic conductivity ratio (C_f) of field to laboratory values is about 6. To analyse the PVD-improved subsoil, a simple approach using the equivalent vertical hydraulic conductivity of PVD-improved subsoil was employed. The analytical results show that PVDs increased the bulk vertical hydraulic conductivity of soft subsoil by about 30 times compared to the original

*Corresponding author. Tel.: +86 021 64191030; fax: +86 21 64191030.
E-mail addresses: slshen@sjtu.edu.cn (S.-L. Shen), chai@cc.saga-u.ac.jp (J.-C. Chai), zshong@seu.edu.cn (Z.-S. Hong), Sam721@sjtu.edu.cn (F.-X. Cai).

doi:10.1016/j.geotexmem.2005.05.002

Nomenclature

C_f	hydraulic conductivity ratio between field and laboratory values
C_v	coefficient of consolidation (L^2/T)
D_e	diameter of unit cell (L)
d_m	equivalent diameter of the cross-sectional area of mandrel (L)
d_s	diameter of smear zone (L)
d_w	diameter of vertical drain (L)
k_s	hydraulic conductivity in the smear zone (L/T)
k_{ve}	equivalent vertical hydraulic conductivity of PVD-improved subsoil (L/T)
l	drainage length (L)
q_w	discharge capacity of PVD in field (L^3/T)
Q_w	discharge capacity of PVD provided by manufacturer (L^3/T)
s	d_s/d_w
S_b	centre to centre spacing between drain (L)
t	thickness of the PVD (L)
w	width of a band-shaped PVD (L)

non-treated subsoil. The discharge capacity of PVDs in this field case is 79–100 m^3/a, which is consistent with the findings from laboratory tests and other reported values in literature.

Keywords: Embankment construction; Soft subsoil; PVD-improvement; FEM analysis; Hydraulic conductivity

1. Introduction

In the design of embankments constructed on soft subsoil, many factors should be considered. One of the most significant aspects is how to reduce the time required for consolidation of soft subsoil. For this purpose, prefabricated vertical drains (PVDs) are often used to accelerate the consolidation of soft subsoils (e.g. Holtz et al., 2001; Bergado et al., 1996; Chai et al., 1996; Hansbo, 1981; Jamiolkowski et al., 1983; Rixner et al., 1986). PVDs can increase the vertical hydraulic conductivity of soft subsoil in a macro-sense by more than one order of magnitude (Bergado et al., 1996; Hansbo, 1981).

FEM has been generally adopted to analyze the behaviour of PVD-improved soft subsoil under embankment loading. There are three existing approaches for modelling the PVD improved subsoil. The first method employs a one-dimensional (1D) drainage element (Chai et al., 1995; Hird et al., 1992; Hird et al., 1995). The second method adopts a macro-element in FEM program to consider the drainage behaviour of vertical drains (Sekiguchi et al., 1986; Zeng and Xie, 1987). The third method is a simple approximate approach, in which an equivalent value of vertical

hydraulic conductivity (k_{ve}) of PVD-improved subsoil is estimated (Chai et al., 2001). Using this approach, the behaviour of PVD-improved subsoil can be analyzed in a similar manner to that of non-treated natural subsoil. Since the third method is simple and can be directly applied in any situation, in this study it was adopted.

The recent economic boom in China has resulted in many new expressways being constructed and Hangzhou–Ningbo (HN) expressway is one of them. HN expressway is located on the southern coast of Hangzhou Bay in the eastern coastal region of China, as shown in Fig. 1. It extends from Hangzhou, the Capital City of Zhejiang Province to Ningbo, which is the biggest harbour city in the same province. The total length of HN expressway is 145 km, of which about 92 km was constructed on soft clay deposits.

In order to better understand the design, construction, and performance of embankments on the soft clay deposits, 12 field full-scale test embankments totally 3.15 km in length were constructed and investigated (TPIZ et al., 1998; Wang, 1998). This paper describes two test embankment sections of HN expressway constructed on soft clay deposits with and without PVD improvement, respectively. The details of these two test sections are provided in Table 1. In the FEM analysis, Chai and Bergado's (1993) technique is adopted to closely simulate the embankment

SPIA = Shanghai Pudong International Airport
NIA = Ningbo International Airport

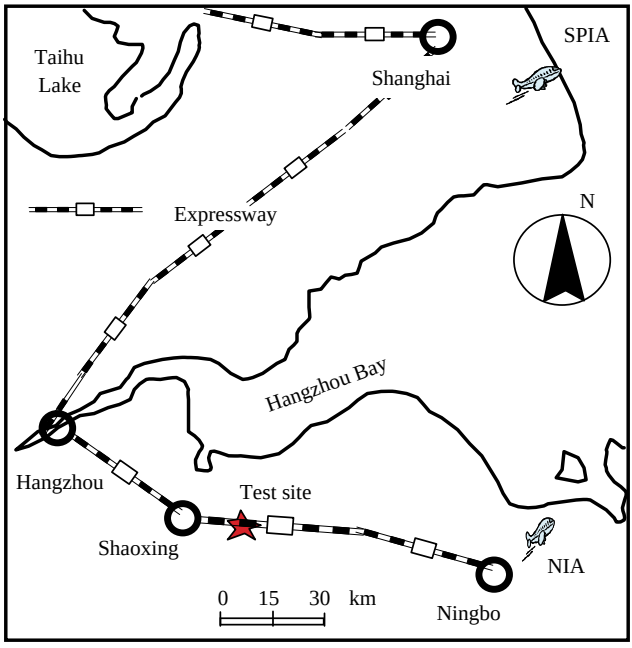

Fig. 1. Location of the test site near Shaoxing in Eastern China.

Table 1
Test embankments with ground improvement descriptions

Embankment cases	H (m)	H_{ps} (m)	n	D_T (m)	D_{clay} (m)	Remarks
T10	4.45	5.88	1:1.5	2.20	23.0	PVD, $t = 6$ mm, $P = 1.5$ m, $D = 19$ m
T11	3.91	4.66	1:1.5	1.05	19.1	Natural subsoil

Note: H = embankment height; H_{ps} = Height of preloading embankment; n = side slope of embankment; D_T = thickness of crust layer; D_{clay} = thickness of clay layer; PVD = plastic drain improved; t = thickness of PVD; P = drain pitch; D = depth of drain.

construction process. Some of the soil parameters were evaluated by back-calculation of the field settlement of the embankment on natural subsoil. For the PVD-improved case, the following influential factors were analyzed and discussed: (i) hydraulic conductivity of subsoil in the field, (ii) discharge capacity of PVDs, and (iii) smear effect. The increase of vertical hydraulic conductivity for PVD-improved subsoil is discussed.

2. Soil conditions

The soil profile and soil properties of the soft clay deposits at the test site are shown in Fig. 2. The soil profile consists of a thin weathered crust (TC) from about 1–1.5 m thick overlying a silty clay (SC1) deposit of approximately 4 m thick. The third layer is very soft clay (MC, in China it is called mucky clay) with a thickness of approximately 10 m for the PVD-improved case and 11.5 m for the unimproved case. Below the clay is a silt clay layer called mucky-silty clay (MSC) approximately 4 m thick for PVD-improved case and 2.7 m for the unimproved case followed by a medium to stiff silty clay layer (SC2) from 3 to 5 m thickness extending down to 23 m depth, which is in turn underlain by a layer of loose clayey sand (CS). The soil layer separation is plotted in Fig. 2, in which solid line denotes the PVD-improved subsoil and dashed line denotes the subsoil without PVD-improvement. The thickness of the soft clay deposit without PVD-improvement is about 19 m and that with PVD-improvement is about 23 m. The soft silt clay and very soft clay have water contents greater than their liquid limits, low hydraulic conductivity and lower shear strength. The parameters such as compression index (C_c) and hydraulic conductivity (k) were determined from laboratory oedometer tests; the values of k_h and k_v were obtained from oedometer test results using the samples oriented in horizontal and vertical directions, respectively. Shear strength S_u were determined from field vane shear test.

3. Construction of embankments and field monitoring

Fig. 3 illustrates the cross-section and plan view of the test embankments, arrangement of PVDs, and instrumentations. As seen in Fig. 3, a 0.5 m thick sand

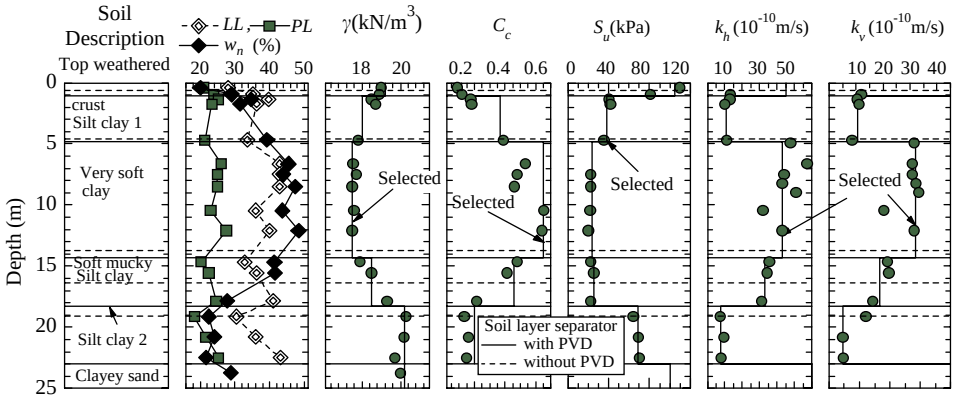

Fig. 2. Soil profile and properties at the test site of thinner deposit section.
Note: LL-liquid limit, PL-plastic limit, w_n-water content, γ-unit weight, C_c-compressive index, S_u-Field vane shear strength, k_h, k_v-hydraulic conductivity in horizontal and vertical direction from laboratory test.

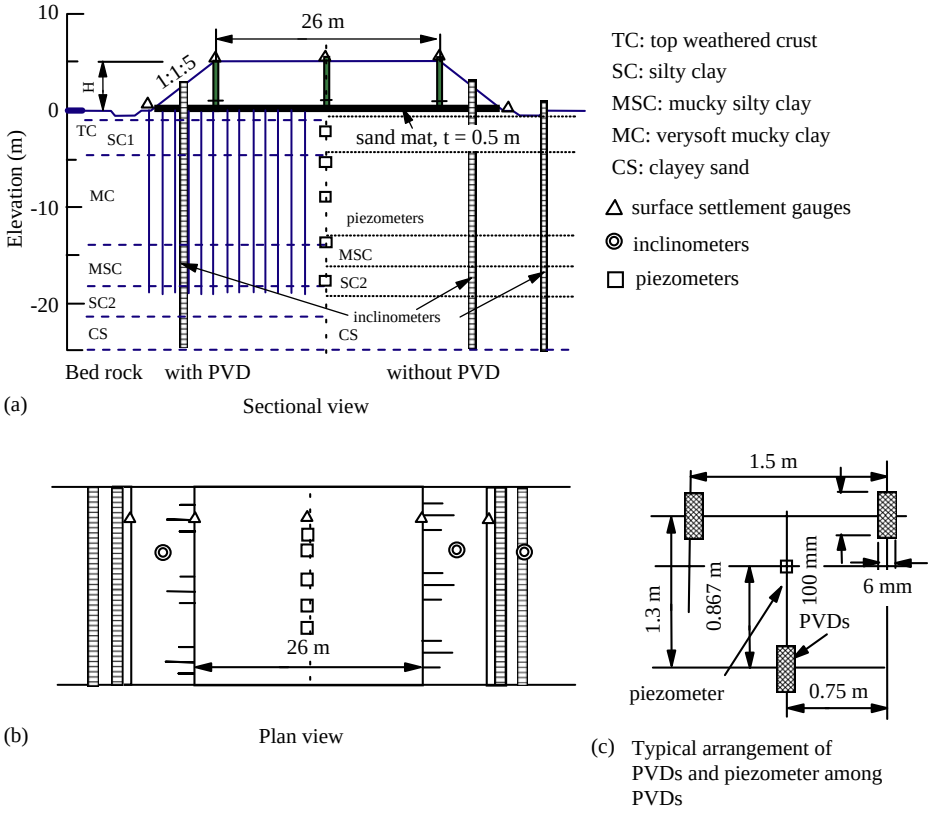

Fig. 3. Cross-section and plan view of embankment, field instrumentation, and arrangement of PVDs in field.

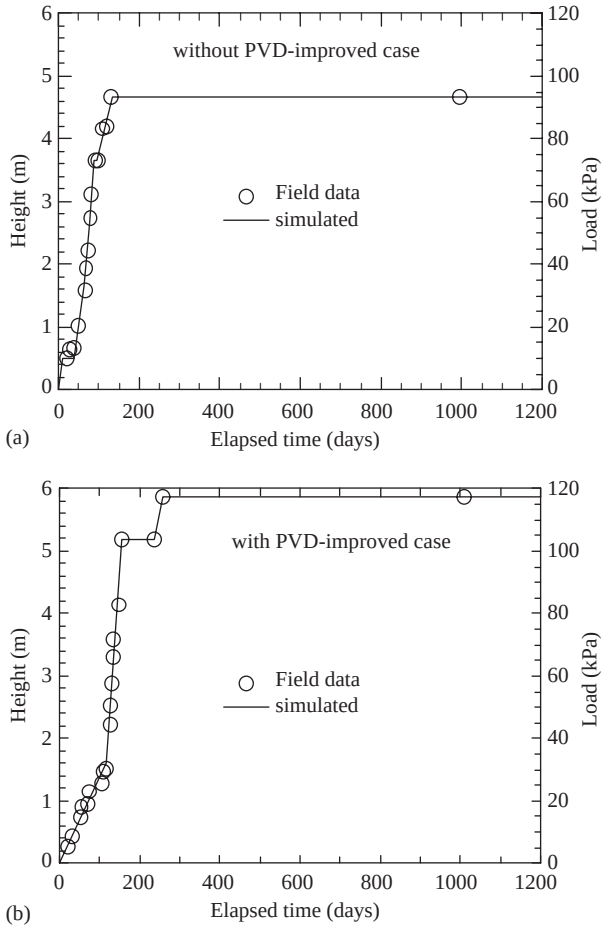

Fig. 4. Load-time history of the embankment on: (a) Natural subsoil; (b) PVD-improved subsoil.

mat (hydraulic conductivity: $k > 0.001$ m/s) was placed on the soft ground initially. Then, decomposed granite was filled and compacted to a unit weight of 20 kN/m^3. The loading-time history relations for the two embankments are plotted in Fig. 4. The height of the embankment on PVD-improved subsoil is 5.88 m and that on natural subsoil is 4.66 m. For the improved case, PVDs were installed in a triangular pattern with the spacing of 1.5–19 m deep. Table 2 lists the properties of PVDs used in the test embankment. The discharge capacity, Q_w, provided by manufacturer is greater than 1500 m^3/year.

Field behaviour of soft ground under embankment loading were observed through monitoring the surface settlement, lateral displacements of the subsoil at the middle point of the embankment side slope, and pore pressure variation by piezometers at different depths. The layout of the field instrumentation is shown in Fig. 3.

Table 2
Size and physical properties of PVDs used in this field project

Thickness (mm)	Width (mm)	Unit weight (g/m)	Q_w (m^3/a)	Material	
				Filter	Core
6	100	108	1580	Nonwoven polyolefin	Corrugated polyethylene

Note: Q_w = discharge capacity of PVD, the value in table was provided by manufacturer.

Table 3
C_f value for some clay deposits

Deposit	C_f	Method	Reference
Bangkok clay (100 km from sea)	25	Back calculated	Chai et al. (1995)
Bangkok clay (close to sea)	4	Back calculated	Chai et al. (1996)
Malaysia Muar clay deposit	2	Back calculated	Chai and Bergado (1993)
Ariake clay	4	Back calculated	Chai and Miura (1999)
Louiseville (Canada)	1	Self-boring permeameter	Tavenas et al. (1986)
St-Alban (Canada)	3	Self-boring permeameter	Tavenas et al. (1986)
Very soft mucky clay (China)	6	Back calculated	Present study

Note: C_f = Ratio between field horizontal hydraulic conductivity k_h value to laboratory value.

4. Field hydraulic conductivity

The hydraulic conductivity of subsoil in the field is different from the laboratory measured value, esp. calculated from laboratory oedometer test result. Laboratory test normally underestimates the field values (Tavenas et al., 1986). The relation can be expressed as following formula:

$$(k_h)_f = C_f(k_h)_l \text{ or } (k_v)_f = C_f(k_v)_l, \tag{1}$$

where k_h, k_v = hydraulic conductivity in horizontal and vertical directions of soil layer, respectively; subscript f and l represent the value in field and the value determined in the laboratory test, respectively; and C_f = hydraulic conductivity ratio between the field and the corresponding laboratory values.

Tavenas et al. (1986) demonstrated that for homogeneous deposit, C_f value is close to 1.0, however, for stratified deposits, even those with thin sand lenses that cannot be clearly identified from the borehole record, C_f value can be much larger than 1.0. The C_f values of a few clay deposits are listed in Table 3 for reference. Field hydraulic conductivity can be measured using a self-boring permeameter in field. However, if there is no available of this equipment, back-calculation of the measured settlement of embankment on natural subsoil is a best way as suggested by Chai and Miura (1999). In this study, back-calculation method was employed to evaluate C_f.

For this field case $C_f = 6$ obtained, and the details will be discussed in the following context.

5. Modelling parameters of PVD-improved subsoil

5.1. Equivalent hydraulic conductivity

According to Chai et al. (2001), the equivalent vertical hydraulic conductivity of PVD improved subsoil, k_{ve}, can be expressed as

$$k_{ve} = \left(1 + \frac{2.5l^2}{\mu D_e^2}\frac{k_h}{k_v}\right)k_v, \tag{2}$$

where l = drainage length; D_e = equivalent diameter of a unit cell (a cylinder contains a PVD and its influential zone) (Balaam and Booker, 1985); for triangle arrangement of PVDs, $D_e = 1.05S_b$, in which S_b is the spacing between two PVDs. And parameter μ can be expressed as follows (Hansbo, 1981):

$$\mu = \ln\frac{n}{s} + \frac{k_h}{k_s}\ln(s) - \frac{3}{4} + \pi\frac{2l^2k_h}{3q_w}, \tag{3}$$

where $n = D_e/d_w$ (d_w = diameter of vertical drain); $s = d_s/d_w$ (d_s = diameter of smear zone); k_s = horizontal hydraulic conductivity in the smear zone; and q_w = discharge capacity of PVD in the field. As shown in Eq. (3), by using parameter μ, well resistance and smear effect can be taken into consideration in the adopted method. One of the deficits of this simple method is that it can not consider the variation of hydraulic conductivity in the smear zone.

5.2. Parameters related to PVD behaviour

The parameters for PVDs are listed in Table 4 and the determination methods are presented as follows.

Table 4
Parameters related to the behaviour of PVD

Item	Symbol	Value
Drain diameter (mm)	d_w	53.0
Ratio of k_h over k_s in laboratory test	$(k_h/k_s)_l$	2.25
Ratio of field k_h value to laboratory value	C_f	6.0
Ratio of k_h over k_s in field	$(k_h/k_s)_f$	13.5
Smear zone diameter (m)	d_s	355
d_s/d_w	s	6.7
Diameter of influential zone (m)	D_e	1.575
D_e/d_w	n	29.7
Discharge capacity (m^3/a)	q_w	100

5.2.1. Equivalent drain diameter

The modified approach for equivalent drain diameter (d_w) of a band-shaped PVD by considering the corner effect is used in this study. It can be calculated using the following equation (Rixner et al., 1986):

$$d_w = \frac{w + t}{2}, \tag{4}$$

where w = width of a band-shaped PVD and t = thickness of the PVD.

5.2.2. Smear effect

When a PVD is installed in soft clay ground using a mandrel, a disturbed zone called smear zone around the mandrel is created, in which the hydraulic conductivity is reduced significantly. There are two parameters needed to evaluate the smear effect, namely, (i) the diameter of the smear zone (d_s) and (ii) the hydraulic conductivity ratio $(k_h/k_s)_f$, i.e., the value in the undisturbed zone (k_h) over that in the smear zone (k_s).

The diameter of the smear zone d_s varied with the different soil type based on several field and laboratory test results (Jamiolkowski et al., 1983; Hansbo, 1987; Hird and Moseley, 2000; Madhav et al., 1993). Jamiolkowski et al. (1983) proposed an equation for calculating d_s is as follows:

$$d_s = (2 \text{ to } 3)d_m, \tag{5}$$

where d_m = equivalent diameter of the cross-sectional area of mandrel. Chai and Miura (1999) suggested that the value of $d_s = 3d_m$ can be used in practice when there are no test data for evaluating the smear zone size. Following their method, $d_s = 3d_m$ is adopted in this study.

Many uncertainty factors affect the value of $(k_h/k_s)_f$ in field. Chai and Miura (1999) proposed the following equation to evaluate this value.

$$\left(\frac{k_h}{k_s}\right)_f = C_f \left(\frac{k_h}{k_s}\right)_l, \tag{6}$$

where k_s = hydraulic conductivity in smear zone; and the other symbols are the same as presented before.

The hydraulic conductivity in smear zone varies with the radius from the centee of PVD. From laboratory test on various clay samples, the average values of $(k_h/k_s)_l$ varies from 1 to 5 (Hansbo, 1987). For Ariake clay it is about 2.5 (Madhav et al., 1993); for preconlidated kaolin clay, the ratio is about 3 (Hird and Moseley, 2000). However, for this particular soil in this study, there is no available laboratory test value. Zhu et al. (1992) reported a case history of sand drain improved subsoil under the runway of Ninbo International Airport (see Fig. 1), where is about 100 km away from the test site in this study. They estimated the value of $(k_h/k_s)_f$ in field of about 12–15. Thus, due to $C_f = 6$, according to Eq. (6), $(k_h/k_s)_l = 2-2.5$ can be evaluated.

5.2.3. Discharge capacity of PVDs

Discharge capacity denotes well resistance of PVDs quantitatively. The discharge capacity of PVDs in field is much lower than the value given by manufacturer (Miura and Chai, 2000; Chai et al., 2004a). Under confined pressure, typical values of discharge capacity, q_w, of many PVDs are from 100 to 500 m^3/year (Holtz et al., 1991). Laboratory test results (Holtz et al., 1991) and theoretical analysis (Li and Rowe, 2001) confirmed that when the discharge capacity is greater than 100–150 m^3/year, there is no significant effect on the consolidation rate. Moreover, discharge capacity will decrease in filed due to following factors (Holtz et al., 1991; Li and Rowe, 2001; Miura and Chai, 2000): (a) confining the drain by clay; (b) effects of air bubble trapped in the drainage path; (c) effects of folding of the drain; (d) clogging by clay particles; and (e) creep of drain filter. Based on the test results, the discharge capacity of some PVD products can be as low as 5–100 m^3/year under high confining pressure and low hydraulic gradients (Holtz et al., 1991). Chai et al. (2004a) and Miura and Chai (2000) showed that long-term discharge capacity of several PVDs confined in clay is about 5–10% of that for short-term confined in a rubber membrane. In this case, the value of discharge capacity in the field (q_w) is from 79 to 100 m^3/a with respect to $(k_h/k_s)_f = 15-12$. And this aspect will be discussed in the following context in certain details.

5.2.4. Effect of sand mat

Part or all of the water collected by PVDs flows to the ground surface first, and then drains out by the outlet system — the sand mat. The hydraulic conductivity of the sand mat affects the analytical results. Although it is related to the scale of an embankment and the depth and the hydraulic conductivity of subsoil, Chai and Miura (1999) showed numerically that for most cases, if the hydraulic conductivity of the sand mat is greater than 10^{-4} m/s, the free drainage path assumption for the sand mat is acceptable. In the present study, the hydraulic conductivity of the sand mat is about 10^{-3} m/s, which is greater than 10^{-4} m/s, so that the free drainage assumption was used in this study.

With the aforementioned parameters, the equivalent hydraulic conductivity (k_{ve}) values for the PVD improved subsoil were calculated from Eq. (2). The results are listed in Table 5. The hydraulic conductivity of PVD-improved subsoil is increased about 30 times.

6. Other modelling aspects in FEM analysis

6.1. Modelling of large deformation problems

The response of soft subsoil under embankment loading is generally analyzed by using FEM (e.g. Chai and Bergado, 1993; Hird et al., 1992; Sun and Wang, 1988). The analysis of embankments on soft subsoil is a large deformation problem since the magnitude of settlement at the end of construction can vary from 20% to 100% of the total settlements (Asaoka et al., 1992; Bergado et al., 1996; Chai and Bergado,

Table 5
Model parameter for subsoil in the test site

Layer	ν	κ	λ	M	e_0	Γ	γ_t (kN/m^3)	k_h (10^{-3} m/d)	k_v (10^{-3} m/d)	k_{ve} (10^{-3} m/d)	k_{ve}/k_v
TC	0.30	0.008	0.08	1.0	0.81	1.98	19.3	2.72	2.72	34.3	12.6
SC1	0.35	0.016	0.16	1.0	1.07	2.22	18.5	0.56	0.22	7.3	33.2
MC	0.35	0.028	0.28	0.8	1.36	3.22	17.3	2.54	1.69	28.9	17.1
SMC	0.35	0.018	0.18	0.8	1.10	2.98	17.9	2.06	1.01	24.1	23.9
SC2	0.30	0.010	0.10	1.0	0.81	1.99	19.3	0.39	0.18	5.2	28.9
CS	0.25	—	—	—	—	—	19.5	25.90	25.90	—	—
Fill	0.20	—	—	—	—	—	20.0	193.5	193.5	—	—

Note: TC = Thin weathered crust; SC = Silty clay; MC = Very soft clay; SMC = soft silty clay; CS = clayey sand; γ_t = unit weight; e_0 = initial void ratio; λ = virgin loading slope in e-ln(p') plot (p' is effective mean stress); κ = reloading/unloading slope in e-ln(p') plot; and M = slope of failure line in p' versus q plot (q is deviator stress); ν = Poisson's ratio.

1993). The large deformation phenomenon can be considered by updating the nodal coordinates during the incremental analysis. Usually, this operation does not include the elements above the current construction level. As a result, the final applied embankment fill thickness will be larger than pre-defined value. There are two methods to treat this problem: (i) include all the embankment elements into all steps of incremental analysis and apply the gravity force by percentage in each step; or (ii) apply the embankment elements layer by layer and correct the coordinate of the elements above the current construction level according to the settlement of the current construction top surface (Chai and Bergado, 1993). This study adopted Chai and Bergado's (1993) proposal.

6.2. Element type and boundary conditions

In FEM analysis, the plain strain condition was assumed. The modelled range in vertical direction was 25 m deep for the case without PVD-improvement and 29 m deep for the case with PVD-improvement; and horizontally 120 m away from the embankment centerline. The displacement boundary conditions were as follows: at bottom, both vertical and horizontal displacements were fixed, and for left and right vertical boundaries, the horizontal displacement was fixed. The adopted drainage boundary conditions were as follows: the ground surface and bottom line (weathered rock) were drained. The left and right boundaries were undrained. Fig. 5 shows the FEM mesh for the embankment on natural subsoil and PVD-improved subsoil. The element type for subsoil and the embankment fill is quadrilateral. Each element has 9 Gauss integral points.

6.3. Constitutive model and parameters

The mechanical behaviour of the soft clay layers was represented by the Modified Cam–Clay model (Roscoe and Burland, 1968) and the clayey sand layer, the sand

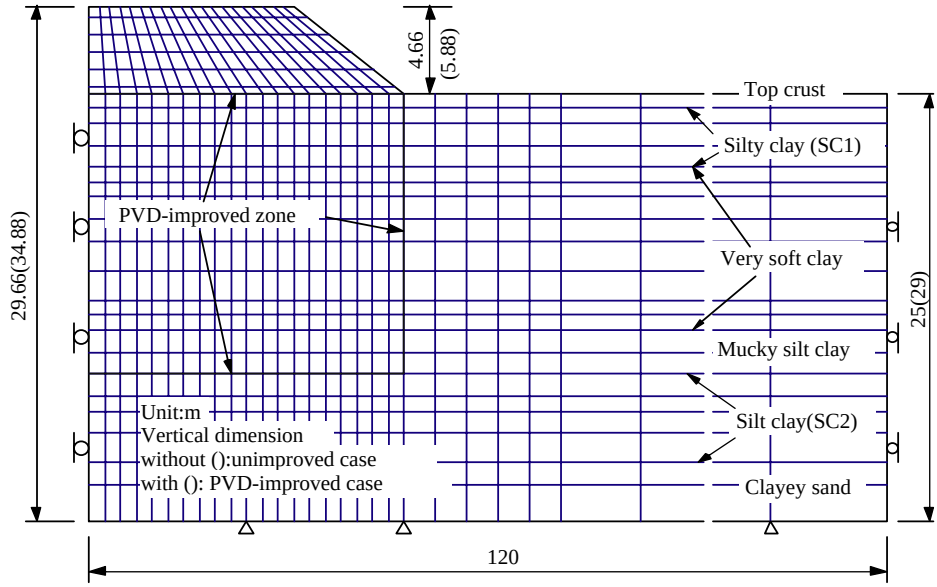

Fig. 5. Finite element analysis mesh.

mat as well as decomposed granite fill material were assumed to be elastic. The determined model parameters for subsoil are listed in Table 5. For the clay layers, the parameters were determined from a standard laboratory oedometer test and triaxial test results on the undisturbed samples (Sun and Wang, 1988), except for Poisson's ratio and hydraulic conductivity. Poisson's ratio, v, was assumed empirically. For the values of hydraulic conductivity, first, the representative laboratory values of $(k_h)_l$ and $(k_v)_l$, which were obtained from standard oedometer test, were selected as shown in Fig. 2. From Fig. 2, the ratio of k_h/k_v was determined to be from 1.5 to 2.5 for the soft clay layers. The results of back-analysis indicate that to fit the measured settlement rate, the field hydraulic conductivities of about 6 times of the selected values in Fig. 2 are required. The adopted field values of hydraulic conductivities, k_h, k_v, are listed in Table 5. The procedure of back-calculation will be presented in the later context. In the analysis, the hydraulic conductivity is also varied with void ratio, e, according to Taylor's equation (Taylor, 1948).

$$k = k_0 \times 10^{-(e_0-e)/C_k}, \tag{7}$$

where, $k_0 =$ initial permeability, $e_0 =$ initial void ratio, $k =$ current value of hydraulic conductivity, $e =$ current void ratio, and $C_k =$ a constant ($= 0.45e_0$, Tavenas et al., 1986).

The subsoil is considered to be in lightly over-consolidated to normally consolidated states with a maximum over-consolidation ratio (OCR) of about 5

for the top crust. The lateral earth pressure coefficient was calculated using the equation proposed by Mayne and Kulhawy (1982).

$$K_0 = (1 - \sin \phi')(\mathrm{OCR})^{\sin \phi'}, \tag{8}$$

where ϕ' is the effective internal friction angle of soil, OCR is over-consolidation ratio.

The parameters for clayey sand were assumed as Young's modulus $E = 25,000\,\mathrm{kPa}$ and Poisson's ratio $v = 0.25$. The mechanical properties of the fill material were assumed as follows: $E = 30,000\,\mathrm{kPa}$ and $v = 0.25$. The unit weight of the fill material was $20\,\mathrm{kN/m^3}$. The ground-water level was about 1.5 m below ground surface.

7. Results and discussions

7.1. Back-calculation of some parameters

The aforementioned parameters such as C_f and q_w were determined from the back-calculation method. The procedure of back-calculation is as follows: (1) Back-calculation of C_f based on the measured settlement of the embankment on natural subsoil; (2) select $(k_\mathrm{h}/k_\mathrm{s})_l = 2-2.5$, using Eq. (5), the field value of $(k_\mathrm{h}/k_\mathrm{s})_f = C_\mathrm{f} \cdot (k_\mathrm{h}/k_\mathrm{s})_l = 12-15$ is obtained; (3) using above values to evaluate the value of q_w in the field from PVD-improved case.

7.1.1. C_f value

C_f was obtained by analyzing the embankment on natural subsoil. In the analysis, the initial values of hydraulic conductivity in Fig. 2 were multiplied by a factor C_f, larger than 1.0 and the calculated settlement was compared with the measured data. The settlement-time relation for the embankment on natural subsoil is plotted in Fig. 6. As shown in the figure, with $C_\mathrm{f} = 6$ (solid line), numerical result agrees well with the measured values. For comparison, the calculated settlement-time curves with respect to $C_\mathrm{f} = 1$ are also plotted using dashed line in the same figure.

7.1.2. Discharge capacity of PVDs

In order to fit the measured data, the discharge capacity of the PVD was varied in the analysis of PVD-improved case. The effect of discharge capacity of PVDs on settlement behaviour is compared in Fig. 7. As illustrated in the figure, the settlement rate of soft subsoil increased with the increase of discharge capacity. When q_w is very small, i.e. less than $10\,\mathrm{m^3/year}$, the calculated value cannot match the field measured data. If q_w is greater than $79\,\mathrm{m^3/year}$, the calculated value can match the field-measured data well. While the q_w is greater than $100\,\mathrm{m^3/year}$ (about 6% of the manufacturer provided value), there is no much effect on the settlement behaviour. Even if the $q_\mathrm{w} = 1500\mathrm{m^3/a}$, there is no much increase of settlement rate. The effect of q_w on behaviour of excess pore pressure was found to be similar to that on

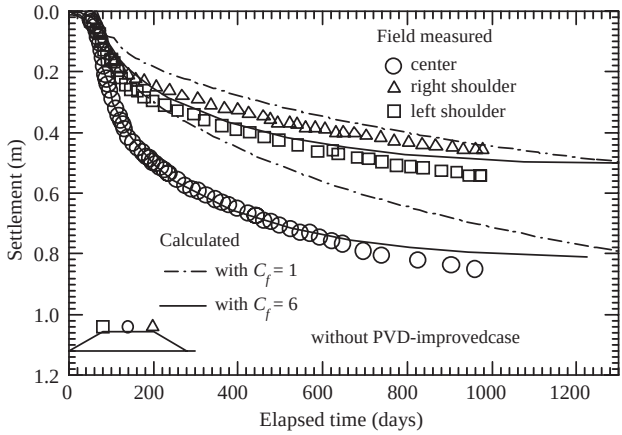

Fig. 6. Measured and calculated values of settlement for the embankments on the subsoil without PVD-improvement.

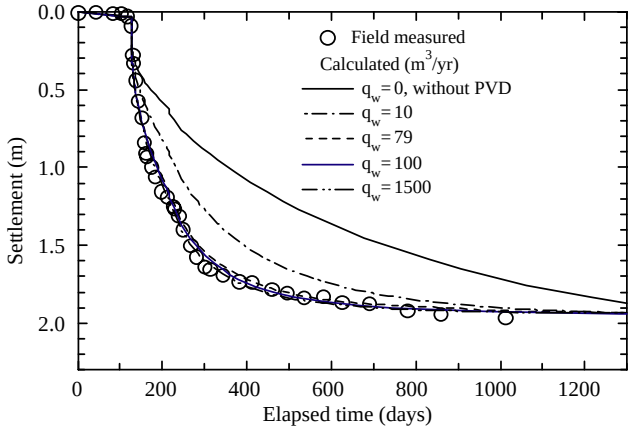

Fig. 7. Effect of discharge capacity of PVDs on the settlement behaviour.

settlement, and the results were plotted in Fig. 8. It can be considered that since the hydraulic conductivity of soft clay is relatively low, when q_w is larger than a certain value, the hydraulic conductivity of soft clay controls the consolidation process rather than q_w. Only with this information, it can be concluded that the field q_w value was larger than 79 m^3/year. However, referring to other reported field values (Holtz et al. 1991; Li and Rowe, 2001), it is considered that q_w values in the filed was about 79–100 m^3/year. The final adopted values are $(k_h/k_s)_f = 13.5$ and $q_w = 100\,m^3/a$. The final calculated settlement-time relation for the embankment on PVD-improved subsoil is plotted in Fig. 9.

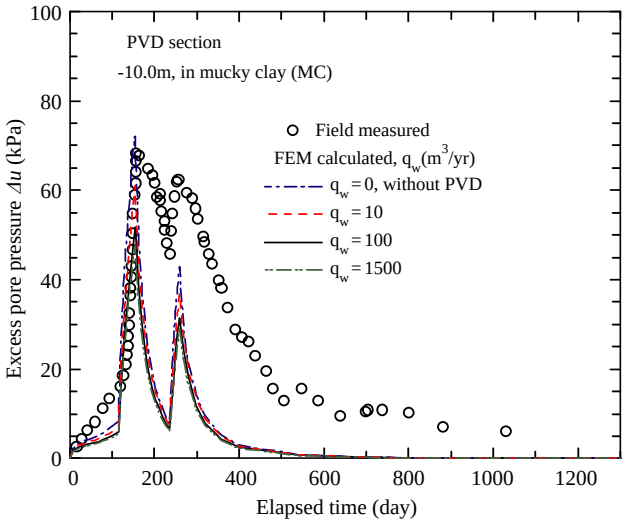

Fig. 8. Variation of calculated excess pore pressure with discharge capacity q_w.

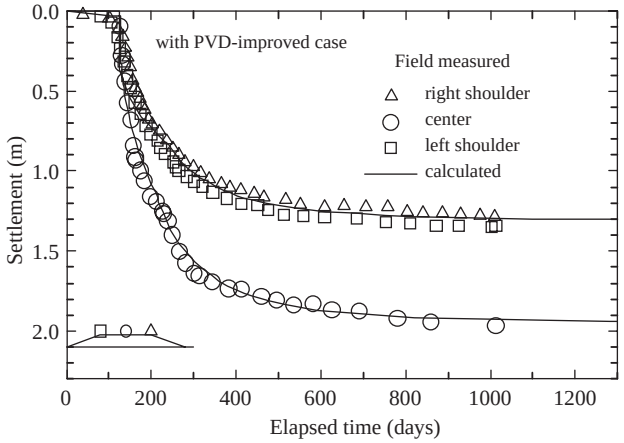

Fig. 9. Measured and calculated values of settlement for the embankments without PVD-improvement.

7.2. *Pore water pressure*

Fig. 10 shows the observed excess pore pressures during embankment construction, which are presented as a function of the applied stress of the embankment at the ground surface. As shown in Fig. 10a, for the embankment on natural subsoil, the generation of pore pressure supports the tendency found by Tavenas and Leroueil (1980), that is, two phases of pore pressure response during construction can be identified: the first, during which the increases in pore pressure are low; the

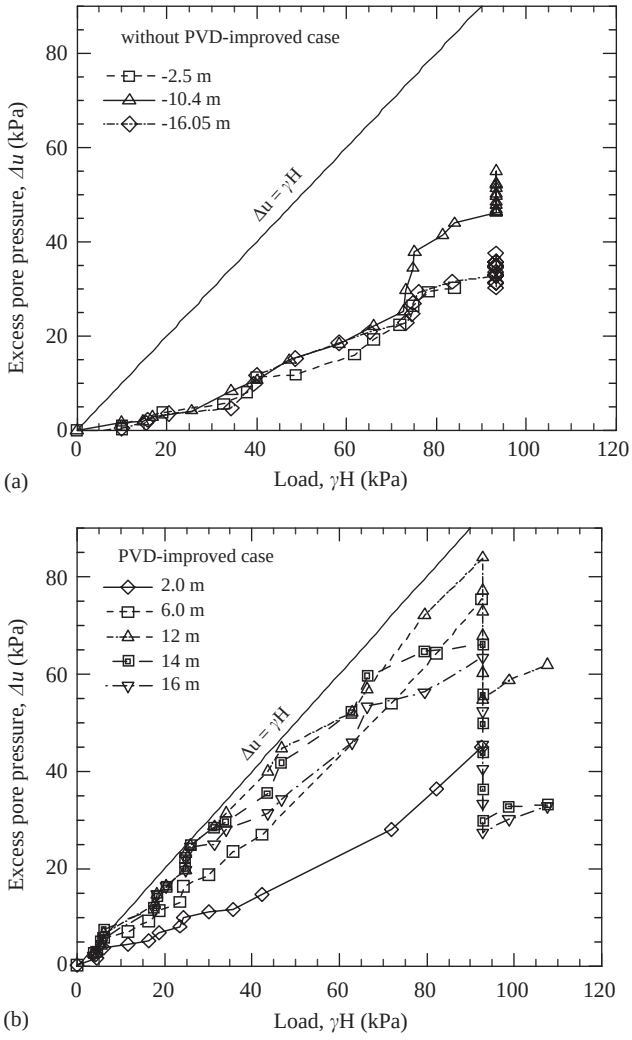

Fig. 10. Pore pressures measured under the centre of the embankment test section, as a function of the embankment load: (a) without PVD-improved case; (b) with PVD-improved case.

second, during which the increase in pore pressures is approximately equal to the increase in total stress. For the embankment constructed on PVD-improved subsoil, the measured pore pressure at a depth of 2 and 6 m still follows the findings of Tavenas and Leroueil (1980). This is because subsoil is partially drained and clay begins to consolidation at the very low pressure during construction (Leroueil et al., 1990). After the embankment pressure is approximately equal to the consolidation yield stress, σ'_p, of the soil. The soil becomes normally consolidated, and now posses a coefficient of consolidation much lower than in the overconsolidated region, and it

behaves essentially as undrained soil (Leroueil et al., 1990). However, the measured pore pressures at deeper place did not agree with this tendency (see Fig. 10b). The detailed discussion on the change of coefficient of consolidation, C_v, with consolidation pressure will be discussed in the later context (see Fig. 12).

This phenomenon may be related to the following factors: (i) disturbance of subsoil during installing PVDs; (ii) reduction of *consolidation yield stress* of crust layer; (iii) piezometers might be installed within the smear zone. In this site, there is a weathered top crust layer, which has much higher strength (about 5 times the soft layer) and stiffness, as shown in Fig. 2. The stiff top crust may tend to distribute the loading from the embankment over a larger area and reduce the level of stress to the underlying softer subsoils. Moreover, top crust layer has a very high over-consolidated ratio with OCR = 5 and has a relative high coefficient of consolidation (C_v). However, installing PVDs will disturb the top crust layer, reduce its consolidation yield stress, and thus reduce C_v value. Hence, the increase of excess pore pressure for the improved case becomes larger than the unimproved case at the early stage of embankment construction in the shallower depth, i.e. less than −6.0 m (see Fig. 10).

The reason for higher excess pore pressure for PVD-improved case in the deeper places ($H > 12$ m) is not clear yet. One of the reasons is that piezometers might be installed in the smear zone. In the field, it is difficult to keep the verticality during PVD installation and boring hole for piezometers installation. Piezometers were designed to be installed at the mid point of PVDs (see Fig. 3). The distance between piezometer and PVD is less than 867 mm. If there is only 2° inclining from vertical direction during installation, the piezometers at 12 m depth will be installed within the smear zone. If piezometers were installed in the smear zone, higher excess pore pressure would be measured.

The comparison of the calculated and measured values of excess pore pressures between PVD-improved case and unimproved case is plotted in Fig. 11. During embankment construction, for the unimproved case, the simulated excess pore pressure agrees the measured value fairly well. However, for the PVD-improved case, the calculated values are much lower than the measured ones. For the both cases, dissipation of calculated excess pore pressures is much faster than that of the measured values.

7.3. Reasons for discrepancies between predicted and measured excess pore pressure

The discrepancy of excess pore pressure between FEM calculated results and field measured data might be due to possible errors in measurement and limitation of calculation methods.

7.3.1. Errors in field measurements

(1) Possible errors of the measured data: Pore pressure is measured by piezomters. Pore water seeps into water chamber through a filter of porous stone. Fine soil particles might infiltrate into the pore of filter to cause ‘‘clogging’’

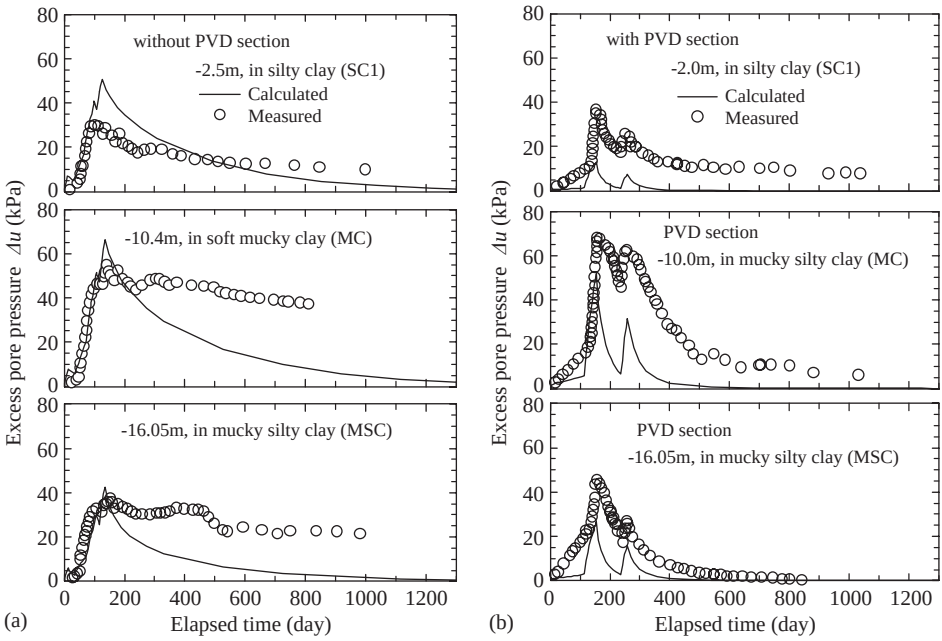

Fig. 11. Measured and calculated excess pore pressure-time curves: (a) without PVD; (b) with PVD.

of the piezomter. Hence, a certain amount of excess pore pressures are "locked in" the piezometer. Some measurements on the excess pore pressure showed that similar behaviour of excess pore pressures was observed, that is, with progressing of consolidation, there were little excess pore pressure dissipations as reported by Chai and Miura (1999), Hird et al. (1995), and Indraratna et al. (1994). For the test embankments on Muar clay, Malaysia, some piezometers showed no excess pore pressure dissipation during the consolidation period. After installing additional piezomters aside the existing points, close to the predicted values of excess pore pressures were measured (MHA, 1989).

(2) Another reason might be that piezometers were installed in smear zone as discussed previously. The modelling method can not simulate this aspect.

7.3.2. *Limitation of calculation methods*

(1) Limitation of modelling method on PVD behaviour: In the field, a single PVD works in a close axisymmetric drainage condition (three-dimensional (3D)). In the present analysis plain strain condition is assumed (two-dimensional (2D) condition) and PVD behaviour is modelled by considering the increased vertical hydraulic conductivity in a macro sense. The equivalent conductivity is obtained

by the average degree of consolidation. The smear effect is taken into account through parameter μ (Eq. (3)) by considering the average hydraulic conductivity, k_s, in smear zone. However, the variation of hydraulic conductivity in smear zone was not taken into account. As a result, local pore pressure distribution in horizontal direction is different between 3D and 2D conditions.

(2) Reduction of q_w value with elapsed time: For discharge capacity, $q_w = 100\,m^3/$ year was used. As discussed in the previous context, increasing q_w will have no effect on the dissipation of excess pore pressure, however, reducing q_w will certainly affect the consolidation rate as illustrated in Fig. 7.

(3) Variation of C_v with consolidation pressure: In this study, the behaviour of soft clay was modelled by Modified Cam–clay model (Roscoe and Burland, 1968). Rising and dissipation of excess pore pressure is related to the coefficient of consolidation C_v. For linear e-ln$p$' relationship, C_v can be expressed as follows:

$$C_v = \frac{(1+e)p'k}{\lambda\gamma_w}, \tag{9}$$

where k = the hydraulic conductivity of soil, γ_w = the unit weight of water, and λ = the slope of virgin compression curve in e-lnp' plot and p' is effective mean stress.

As shown in Eq. (9), C_v, is related to the void ratio, compressive index, stress level, and hydraulic conductivity. Moreover, hydraulic conductivity k varies with the void ratio (Tavenas et al., 1986; Taylor, 1948). Fig. 12 shows a comparison of the calculated values C_v using Eq. (9) and measured C_v for Ariake clay (Chai et al., 2004b). As shown in the figure, even considering the variation of k with e, there are still discrepancies between the calculated values and the measured data.

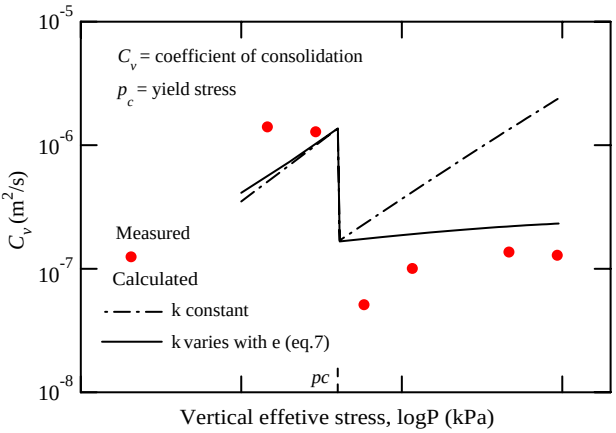

Fig. 12. Variation of the coefficient of consolidation with vertical effective stress (Chai et al., 2004b).

7.4. Settlement

The calculated settlements with the comparison to measured values of the embankment on natural subsoil and PVD-improved subsoil are shown in Fig. 6. FEM can fairly predict the field data. The difference of measured settlements of the two shoulders for each embankment may be due to the non-uniformity of the in situ soils. This aspect was not considered in the FEM analysis. For the PVD-improved case, the primary consolidation was finished in about 600 days, however, for the unimproved case, it need much longer time to finish the primary consolidation. If checking it carefully, we found that in the initial period, the FEM analysis over-estimated the settlement slightly, however, after 600 days, the FEM analysis underestimates the settlement. The reason for the FEM under-prediction of the settlement after 600 days, is that after 600 days, the primary consolidation is essentially completed and secondly compression could not be simulated by the Modified Cam–Clay model.

7.5. Lateral displacement

The calculated and measured values for the lateral displacement are shown in Fig. 13. As illustrated in Fig. 13, the FEM can simulate the profile of lateral displacement very well for the unimproved case. However, there are some discrepancies between measured and simulated ones. Although the lateral displacement at the end of construction for the PVD-improved case is much larger than that for unimproved case, for the same embankment thickness 4.66 m, the calculated lateral displacements are not different much. For the PVD-improved case, at embankment thickness of 5.18 m there was a leaving period of 82 days (see Fig. 4b) and this period might increase the lateral displacement much. If checking Fig. 13 carefully, for PVD-improved subsoil, the measured results show that the place where maximum lateral displacement occurred is about 4 m deeper than that for the unimproved case, however, the calculated values are the same as the unimproved one and about 6 m from the ground surface. The exact reason is not clear but is probably due to the spatial variation of subsoil condition.

8. Conclusions

The following conclusions are based on the field measured data and the associated FEM results:

1. According to the back-calculation of the embankment on natural subsoil, the field hydraulic conductivity is about 6 times the laboratory test values of soft clay deposit at the test site.
2. The evaluated field discharge capacity is greater than 79–100 m^3/a. This value is consistent with the laboratory test data and other reported field values.

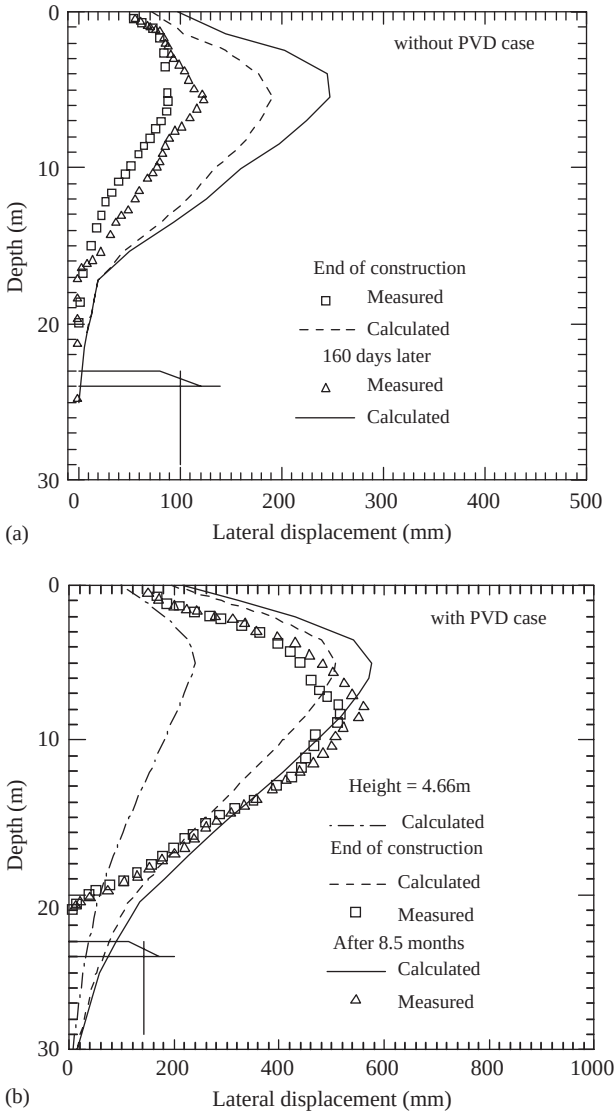

Fig. 13. Measured and calculated lateral displacement: (a) without PVD; (b) with PVD.

3. In the macro-sense, installation of PVD with the spacing of 1.5 m makes increased the vertical bulk hydraulic conductivity of the soft subsoils by about 30 times compared to that for the untreated soil.
4. During embankment construction, the excess pore pressure measured for PVD-improved subsoil were quite different from those without PVD-improvement. The rapid increase in the excess pore pressure at shallower depths for PVD-improved subsoil may be due to disturbance arising from PVD installation.

References

Asaoka, A., Nakano, M., Matsuo, M., 1992. Prediction of partially drained behavior of soft clays under embankment loading. Soils and Foundations 32, 41–58.

Balaam, N.P., Booker, J.R., 1985. Analysis of rigid rafts supported by granular piles. International Journal for Numerical and Analytical Methods in Geomechanics 5, 379–403.

Bergado, D.T., Anderson, L.R., Miura, N., Balasubramaniam, A.S., 1996. Soft Ground Improvement, in Lowland and other Environments. ASCE Press, pp. 427.

Chai, J.C., Bergado, D.T., 1993. Some techniques for FE analysis of embankment on soft ground. Canadian Geotechnical Journal 30 (4), 710–719.

Chai, J.C., Miura, N., 1999. Investigation of factors affecting vertical drain behavior. Journal of Geotechnical and Geoenvironmental Engineering 125 (3), 216–226.

Chai, J.C., Miura, N., Sakajo, S., Bergado, D.T., 1995. Behaviour of vertical drain improved subsoil under embankment loading. Soils and Foundations 35 (4), 49–61.

Chai, J.C., Bergado, D.T., Miura, N., Sakajo, S., 1996. Back calculated field effect of vertical drain. Proceedings of the second International Conference Soft Soil Engineering. Hohai University, Nanjing, vol. 1, pp. 270–275.

Chai, J.C., Shen, S.L., Miura, N., Bergado, D.T., 2001. A simple method of modeling PVD improved subsoil. Journal of Geotechnical and Geoenvironmental Engineering 127 (11), 965–972.

Chai, J.C., Miura, N., Nomura, T., 2004a. Effect of hydraulic radius on long-term drainage capacity of geosynthetics drains. Geotextiles and Geomembranes 22, 3–16.

Chai, J.C., Miura, N., Zhu, H.H., Yudhbir, 2004b. Compression and consolidation characteristics of structured natural clay. Canadian Geotechnical Journal 41 (12), 1250–1258.

Hansbo, S., 1981. Consolidation of fine-grained soils by prefabricated drains. Proceedings of the Tenth International Conference on Soil Mechanics and Foundation Engineering, Stockholm, 3, pp. 677–682.

Hansbo, S., 1987. Design aspects of vertical drains and lime column installations. Proceedings of Ninth Southeast Asian Geotechnical Conference. Southeast Asian Geotechnical Society, Bangkok, vol. 2(8), pp. 1–12.

Hird, C.C., Moseley, V.J., 2000. Model study of seepage in smear zones around vertical drains in layered soil. Geotechnique 50 (1), 89–97.

Hird, C.C., Pyrah, I.C., Russell, D., 1992. Finite element modelling of vertical drains beneath embankments on soft ground. Geotechnique 42 (3), 499–511.

Hird, C.C., Pyrah, I.C., Russell, D., Cinicioglu, F., 1995. Modelling the effect of vertical drains in two-dimensional finite element analyses of embankments on soft ground. Canadian Geotechnical Journal 32, 795–807.

Holtz, R.D., Lancellotta, R., Jamiolkowski, M., Pedroni, S., 1991. Laboratory testing of prefabricated "wick" drains. Proceedings of Geo-Coast'91, Yokohama, Japan, pp. 311–316.

Holtz, R.D., Shang, J.Q., Bergado, D.T., 2001. Soil improvement. Geotechnical and Geoenvironmental Engineering Handbook. Kluwer Academic Publishing, Norwell, USA, pp. 429–462 (Chapter 15).

Indraratna, B., Balasubramaniam, A.S., Ratnayake, P., 1994. Performance of embankment stabilized with vertical drains on soft clay. Journal Geotechnical Engineering 120 (2), 257–273.

Jamiolkowski, M., Lancellotta, R., Wolski, W., 1983. Pre-compression and speeding up consolidation, general report. Special Session 6, Proceedings of Eight European Conference on Soil Mechanics and Foundation Engineering. Balkema, Rotterdam, pp. 1201–1226.

Leroueil, S., Magnan, J.P., Tavenas, F., 1990. Embankments on soft clays. English Edition, translated by D.M. Wood. Ellis Horwood, New York, 360pp.

Li, A.L., Rowe, R.K., 2001. Combined effects of reinforcement and prefabricated vertical drains on embankment performance. Canadian Geotechnical Journal 38 (1), 1266–1282.

Madhav, R., Park, Y.M., Miura, N., 1993. Modelling and study of smear zones around band shaped drains. Soils and Foundations 33 (4), 135–147.

Mayne, P.W., Kulhawy, F.H., 1982. K_0-OCR relationships in soils. Journal of Geotechnical Engineering 108 (GT6), 851–872.

MHA, Malaysian Highway Authority. 1989. Proceedings of Internayional Symposium on Trial Embankments on Malaysian Marine Clays, vol. 1.

Miura, N., Chai, J.C., 2000. Discharge capacity of prefabricated vertical drains confined in clay. Geosynthetics International 7 (2), 119–135.

Rixner, J.J., Kraemer, S.R., Smith, A.D., 1986. Prefabricated vertical drains. Engineering Guidelines, FWHA/RD-86/168, Federal Highway Administration, Washington DC, vol. 1.

Roscoe, K.H., Burland, J.B., 1968. On the generalized stress-strain behavior of 'wet' clay. In: Heyman, J., Leckie, F.A. (Eds.), Engineering Plasticity. Cambridge University Press, Cambridge, UK, pp. 535–609.

Sekiguchi, H., Shibata, T., Fujimoto, A., Yamaguchi, H., 1986. A macro-element approach to analyzing the plain strain behavior of soft foundation with vertical drains. Proceedings of Thirty-first National Conference, JGS, pp. 111–116 (in Japanese).

Sun, J., Wang, B.J., 1988. Finite Element Analysis in Geotechnical Engineering. Tongji University Press, Shanghai (in Chinese).

Tavenas, F., Leroueil, S., 1980. The behaviour of embankments on clay foundations. Canadian Geotechnical Journal 17, 236–260.

Tavenas, F., Tremblay, M., Larouche, G., Leroieil, S., 1986. In-situ measurement of permeability in soft clays. ASCE Special Conference on Use of In-situ Tests in Geotechnical Engineering. ASCE, New York, pp. 1034–1048.

Taylor, D.W., 1948. Fundamentals of Soil Mechanics. Wiley, New York.

Transportation Planning Institute of Zhejiang (TPIZ). Zhejiang University, Fourth Survey Institute of the Ministry of Railway, 1998. Field investigation on the soft ground treatment of Hangzhou-Ningbo (HN) expressway foundation. In: Cai, T.-L. (Ed.), Soft Ground Treatment in HN Expressway. Hangzhou Press, Hangzhou, pp. 21–158 (in Chinese).

Wang, Y.H., 1998. Report on the soft ground treatment of Hangzhou-Ningbo (HN) expressway foundation of test embankment 7–12. In: Cai, T.-L. (Ed.), Soft Ground Treatment in HN Expressway. Hangzhou Press, Hangzhou, pp. 183–222 (in Chinese).

Zeng, G.X., Xie, K.H., 1987. Consolidation analysis of sand drained ground by FEM. Proceedings Eighth Asian Regional Conference on Soil Mechanics and Foundation Engineering, vol. 1, Kyoto, pp. 139–142.

Zhu, X.R., Pan, Q.Y., Bian, S.Z., Xie, K.H., 1992. Strengthening of soft clay ground by surcharge preloading of Ningbo International Airport. Chinese Journal of Geotechnical Engineering 14 (Suppl.), 30–38 (in Chinese).